Parameterization and Impact of Ice Initiation Processes Relevant to Numerical Model Simulations of Cirrus Clouds

PAUL J. DEMOTT, MICHAEL P. MEYERS, AND WILLIAM R. COTTON

Department of Atmospheric Science, Colorado State University, Fort Collins, Colorado

(Manuscript received 3 December 1992, in final form 13 May 1993)

ABSTRACT

An effort to improve descriptions of ice initiation processes of relevance to cirrus clouds for use in regional-scale numerical cloud models with bulk microphysical schemes is described. This is approached by deriving practical parameterizations of the process of ice initiation by homogeneous freezing of cloud and haze (CCN) particles in the atmosphere. The homogeneous freezing formulations may be used with generalized distributions of cloud water and CCN (pure ammonium sulfate assumed). Numerical cloud model sensitivity experiments were made using a microphysical parcel model and a mesoscale cloud model to investigate the impact of the homogeneous freezing process and heterogeneous ice nucleation processes on the formation and makeup of cirrus clouds. These studies point out the critical nature of assumptions made regarding the abundance and character of heterogeneous ice nuclei (IN) present in the upper troposphere. Conclusions regarding the sources of ice crystals in cirrus clouds and the potential impact of human activities on these populations must await further measurements of CCN and particularly IN in upper-tropospheric and lower-stratospheric regions.

1. Introduction

Cirrus clouds occur over wide areas and with high frequency in the atmosphere (Hobbs and Deepak 1981). They also play an important role in the earth's radiation balance (e.g., Cox 1971). Their radiative properties depend to a large extent on the sizes, shapes, concentrations, and phase of cloud particles (e.g., Stephens et al. 1990). The particle size distribution in cirrus clouds is regulated by both cloud dynamics (i.e., ascent, turbulence, and radiative cooling) and the aerosol content of the atmosphere. The link to cloud-active aerosols is through two fundamentally different nucleation processes for ice formation at cold temperatures. Namely, ice crystals may form in cirrus clouds as a result of homogeneous freezing of cloud droplets and haze particles (Sassen and Dodd 1988, 1989; Heymsfield and Sabin 1989; DeMott and Rogers 1990) and heterogeneous nucleation on ice nuclei (IN).

While a number of mesoscale and regional-scale cloud models exist with detailed dynamical frameworks and some include parameterizations of the radiative effects of water and ice phases, few if any contain detailed parameterizations to represent all of the ice initiation processes of relevance to cirrus clouds. One reason for this has been the lack of relevant measurements of cloud condensation nuclei (CCN) and IN. Despite the dearth of measurements, we present herein a framework for parameterizing ice formation in cirrus clouds within mesoscale models. We also investigate, using the best available knowledge, the importance and role of the different ice formation processes using sensitivity simulations with a microphysical parcel model and with a mesoscale cloud model. It is shown that the predicted concentrations, sizes, and spatial distribution of ice crystals depend critically on the assumptions made regarding the abundance of heterogeneous ice nuclei in the upper troposphere, as well as the sizes and supersaturation spectra of CCN.

Corresponding author address: Dr. Paul J. DeMott, Research Associate, Colorado State University, Department of Atmospheric Science, Ft. Collins, CO 80523.

2. Basis for parameterizing homogeneous freezing nucleation

For this study, cloud water and unactivated particles are treated as separate populations. In reality the CCN concentrations, sizes, and compositions will determine the populations of both cloud droplets and haze particles for given atmospheric conditions. Our current treatment is satisfactory for most cloud models using bulk microphysics because cloud droplet activation is not typically treated in detail. This is the current status of the model we are using separately for simulating specific cirrus cloud cases.

a. Homogeneous freezing of supercooled liquid water

The total concentration of cloud droplets freezing in time step Δt may be formulated as

$$N_f = \int_0^\infty (1 - \exp(-J_{ls} V_l \Delta t)) n(D) dD \quad (1)$$

with

$$J_{ls} = J_{ls0}$$

and

$$V_l = \frac{\pi D^3}{6}.$$

The concentration of droplets freezing is determined by the spectral density function of cloud droplets $n(D)$, the volume of the drops V_l, and a formulation for the nucleation rate of pure water J_{ls0}. Since J_{ls0} is primarily a function of droplet temperature (T_l) and is not a function of droplet diameter D, (1) may be easily integrated for a generalized distribution of cloud droplets.

There are a number of approaches to obtaining J_{ls0}. One method is to use a classical theoretical calculation. Assuming equilibrium conditions of a spherical ice embryo in water and using the steady-state approximation of the number of embryos passing critical size (see, for example, Pruppacher and Klett 1978),

$$J_{ls0} = A \exp\{B[\ln(T_o T_l^{-1})]^2\}, \qquad (2)$$

where

$$A = 2N_c\left(\frac{\rho_w k T_l}{\rho_i h}\right)\left(\frac{\sigma_{i-w}^{1/2}}{kT_l}\right)\exp\left(\frac{-\Delta F_{\text{act}}}{kT_l}\right)$$

and

$$B = \frac{-16p\sigma_{i-w}^3}{3kT_l(L_f\rho_i)^2}.$$

In using this approach, one is faced with selecting values for quantities, the true values of which are uncertain, but the impact of which on the calculation can be large. Most critical is the value chosen for the interfacial surface tensions at the ice–water interface (σ_{i-w}). The primary recourse for determining this value has been to use actual experimental data on the freezing of pure water or highly dilute solution droplets. DeMott and Rogers (1990) found a value of $\sigma_{i-w} = 27$ erg cm^{-2} to characterize their data on the freezing of droplets nucleated and freely grown on three types of CCN. Constant values for the latent heat of fusion (L_f) and the activation energy for self diffusion of water (ΔF_{act}), as given by Taborek (1985), were used to obtain this value. Values of N_c and ρ_i were taken from Pruppacher and Klett (1978). Values of J_{ls0} as given by this result are compared with the experimental data in Fig. 1.

Also shown in Fig. 1 are the Sassen and Dodd (1988) estimates for J_{ls0} made by combining numerical calculations with aircraft measurements in high-altitude clouds. They suggested that values for J_{ls0} versus temperature were well described as being about 10^6 times the theoretical values given by Pruppacher and Klett (1978). Such a curve is in good agreement with the curve suggested by DeMott and Rogers. In a theoretical study of homogeneous freezing nucleation and its effect

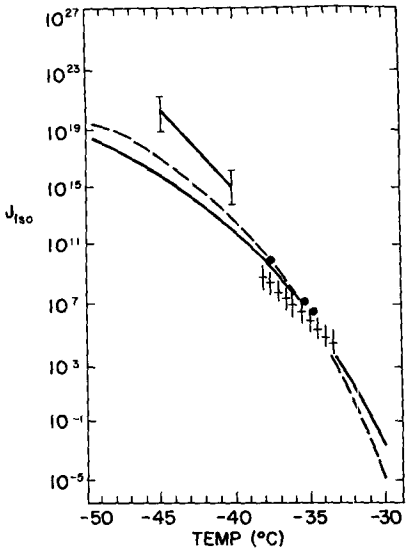

FIG. 1. Homogeneous freezing nucleation rate of pure water J_{ls0} (cm^{-3} s^{-1}) versus temperature. Various estimates shown include experimental data from DeMott and Rogers (1990) (crosses) and Hagen et al. (1981) (bars), field data from Sassen and Dodd (1988) (solid circles), and theoretical approximations from DeMott and Rogers (1990) (solid line) and Heymsfield and Sabin (1989) (dashed).

on cirrus ice crystal formation, Heymsfield and Sabin (1989) used the temperature dependence for J_{ls0} given by Eadie's (1971) statistical thermodynamic model for water. This could be approximated as (Heymsfield and Milosevich 1993)

$$J_{ls0} = 10^y, \qquad (3)$$

where

$$y = -606.3952 - (52.6611Tc) - (1.7439Tc^2) - (0.0265Tc^3) - (1.536 \times 10^{-4}Tc^4)$$

for T_c ($=T_l - 273$) ≤ -50°C. This function is shown by the dashed line in Fig. 1. This result is also in excellent agreement with DeMott and Rogers (1990) and Sassen and Dodd (1988) over the temperature range of their measurements, and lends support to these. However, Eadie's curve diverges to higher values than the others at temperatures below −45°C. In this sense, it is in better agreement with the rapid expansion experiments quantified by Hagen et al. (1981), which provide data for pure water droplets below −40°C. For these reasons and for its simplicity, (3) is used for pure water in the numerical part of this study.

b. *Homogeneous freezing of CCN solution droplets*

In many cases, cirrus ice crystals may form at temperatures below −38°C and below water saturation where freezing can occur on solution droplets or haze particles. In this case, J_{ls} replaces J_{ls0} in (1), where J_{ls} is now a function of both dry particle size (Ds) and

the water vapor saturation ratio (Sw) with respect to water, in addition to temperature. Also, V_l is now $\pi Da^3/6$, where Da is the solution droplet diameter (replacing D).

The theoretical approach to calculating J_{ls} is straightforward, but is repeated here for discussion purposes. Following Pruppacher and Klett (1978),

$$J_{ls} = A \exp\{B[\ln(T_o T_l^{-1} a_w^{(RT_{ol}/M_w L_f)})]^2\}, \quad (4)$$

where

$$a_w = \exp(-0.001 \nu \phi_s M_w M).$$

In this formulation, any solution effects on the preexponential factor A, σ_{i-w} in particular, are ignored. This equation differs from (2) only by the factor including water activity a_w. Water activity will always be less than 1, so the effect of the solution is a depression of the melting point temperature.

This purely theoretical approach is not entirely satisfactory for developing a parameterization because the effects of the solution concentrations on homogeneous freezing rates are underpredicted. Due to nonideal ionic interactions between the solute and condensed water, the freezing point is depressed an amount in addition to the amount obtained by considering curvature (Kelvin) and equilibrium solution (Raoult) effects (i.e., Pruppacher and Klett 1978, 280–281). Sassen and Dodd (1988) therefore formulated an effective freezing temperature as

$$T^* = T_l + (1.7\Delta T_m). \quad (5)$$

This equation was based on Rassmussen's (1982) observations of the relationship between the depression of nucleation temperature and the melting point depression for a variety of salt solutions. This point is reemphasized here because the neglect of such a relationship could lead to very large overestimates of homogeneous freezing nucleation rates of solution droplets.

Table 1 gives some values of J_{ls} from −40° to −50°C at 95% relative humidity for four mass categories of pure ammonium sulfate CCN as calculated with (4) and as calculated by substituting (5) in (3). In a procedure similar to that used by Heymsfield and Sabin (1989), we evaluated ΔT_m for ammonium sulfate [$(NH_4)_2SO_4$] based on Weast (1981) as

$$\Delta T_m = 0.102453 + (3.48484)M, \quad (6)$$

valid from $M = 0.038$ to 3.716 ($r^2 = 0.9996$). Molality is evaluated as

$$M = \frac{1000 m_s}{M_s[(\pi D_a^3 \rho_l'')/6 - m_s]}, \quad (7)$$

where ρ_l'' is solution density and m_s the dry solute mass. Unique values for D_a, M, and ρ_l'' were obtained by solving the well-known Kohler equation,

TABLE 1. Freezing nucleation rate for ideal and nonideal solution effects at $S_w = 0.95$.

T (°C)	m_s (g)	J_{ls} (cm^{-3} s^{-1})	J_{ls0} (T^*)
−40.0	1.0×10^{-16}	5.3	6.0×10^{-32}
	1.0×10^{-15}	3.3×10^{4}	8.3×10^{-12}
	1.0×10^{-14}	6.4×10^{5}	2.8×10^{-6}
	1.0×10^{-13}	2.1×10^{6}	3.4×10^{-4}
−45.0	1.0×10^{-16}	1.7×10^{8}	1.1×10^{-9}
	1.0×10^{-15}	5.7×10^{10}	4.2×10^{2}
	1.0×10^{-14}	4.3×10^{11}	6.3×10^{5}
	1.0×10^{-13}	9.5×10^{11}	8.8×10^{6}
−50.0	1.0×10^{-16}	1.4×10^{13}	2.4×10^{3}
	1.0×10^{-15}	8.7×10^{14}	2.2×10^{10}
	1.0×10^{-14}	3.5×10^{15}	2.0×10^{12}
	1.0×10^{-13}	6.2×10^{15}	1.2×10^{13}

$$\ln S_w = \frac{4 M_w \sigma_{l-a}}{R T_l \rho_w D_a} - \ln a_w, \quad (8)$$

which expresses equilibrium growth conditions for a dry solute particle at a given S_w. Both the interfacial surface tension of the solution–air interface σ_{l-a} and ρ_l'' depend on molality and the particular salt. Empirical relationships for these quantities with ammonium sulfate as the soluble component were obtained from Pruppacher and Klett (1978) and Weast (1981), respectively, as

$$\sigma_{l-a} = 76.10 - 0.155(T_l - 273.15) + 2.17M \quad (9)$$

$$\rho_l'' = 1.0054 + 0.062075M. \quad (10)$$

Based on the results summarized in Table 1, we will use the effective freezing temperature approach as a basis for formulating the solution droplet freezing parameterization. Nevertheless, we must note that no one has yet directly verified freezing rates of haze solution droplets in a laboratory setting.

To circumvent the need to implicitly solve (8), it is possible to develop approximate relations for D_a and M to substitute into the equations for explicitly evaluating (1) for haze particles. What is sought for a mesoscale model parameterization, however, is a simple relation describing the formation of ice directly from a distribution of CCN. Therefore, the system of equations (1), (3), and (5) through (10) were solved for unit mass particles in order to seek a parameterization of N_f. If the haze particles are mixtures of specific soluble and insoluble components, the equations are easily modified by replacing m_s with $\epsilon_m m_n$, where ϵ_m is the soluble mass fraction and m_n is the mixed particle mass. We assume pure ammonium sulfate CCN.

The solid curves in Fig. 2 show the logarithm of the computed fractions freezing F_{hf} (s^{-1}) of haze particles containing given masses m_s of dry CCN at three temperatures. The results shown in Fig. 2 are consistent

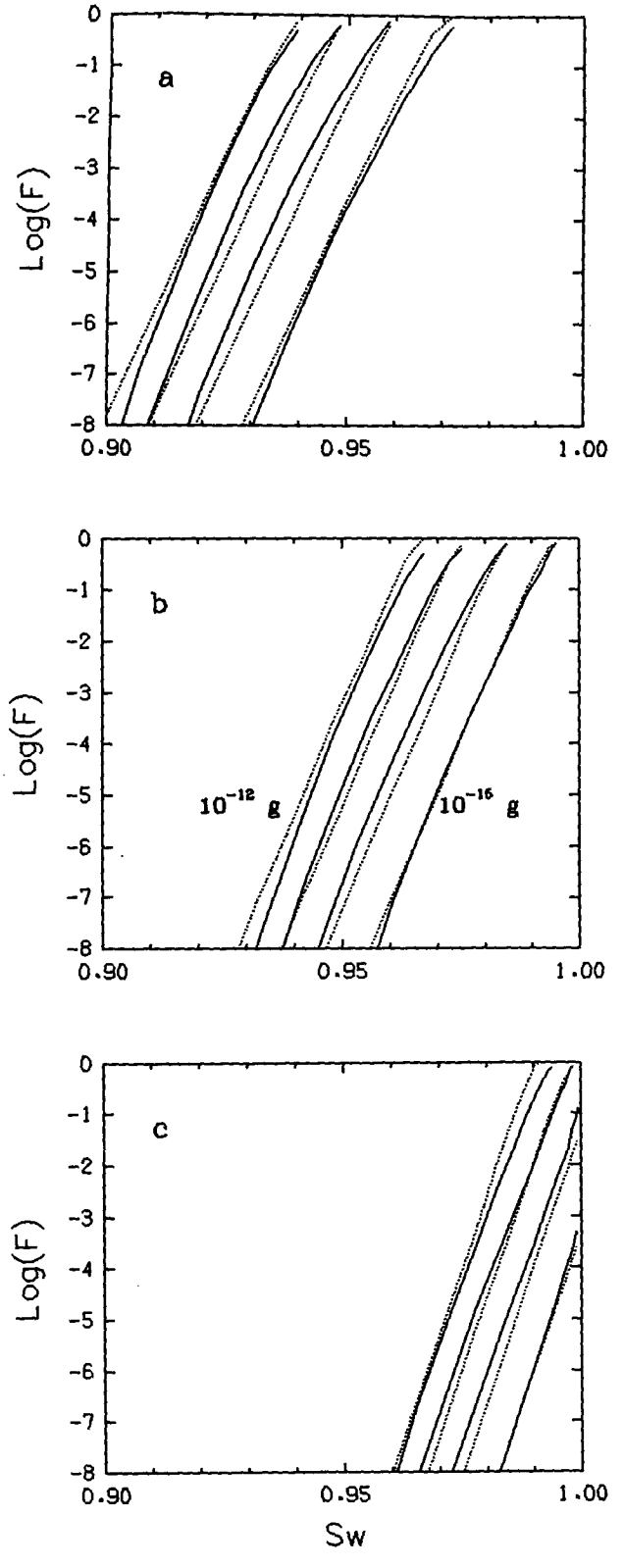

FIG. 2. Logarithms of the fractions of unit mass (10^{-12} to 10^{-15} g), pure ammonium sulfate aerosols nucleating ice as a function of saturation ratio at −50°C (a), −45°C (b), and −40°C (c). Solid lines are exact and dotted lines parameterized results.

with Sassen and Dodd's (1989) estimated minimum saturation ratio required for ice initiation. A point not clearly made in previous studies of this type is that curves of constant dry CCN mass (g) appear approximately linear over a wide range of $\log F_{hf}$. They asymptotically approach $F_{hf} = 0$, however, at low humidity and $F_{hf} = 1$ at high humidity. This observation guided the form of the approximation chosen. The equation derived to approximate the equilibrium behavior of F_{hf} as a function of S_w, spherical dry solute diameter D_s, and T_l is

$$F_{hf} = 1 - \exp(-aD_s^b) \tag{11}$$

with

$$a = \frac{(\pi\rho_s)^2}{6} \times 10^{c1+c2(1-S_w)}$$

$$b = 6.$$

Here $c1$ and $c2$ are functions of solution droplet temperature given by $c1 = -14.65 - [1.045(T_l - 273.16)]$, and $c2 = -492.35 - [8.34(T_l - 273.16)] - [0.061(T_l - 273.16)^2]$. The solute density ($\rho_s$) for ammonium sulfate is 1.769 g cm^{-3}. The results thus parameterized are plotted as dashed curves in Fig. 2. Although exact agreement could not be obtained for all sets of conditions, (11) satisfactorily describes homogeneous freezing nucleation by a distribution of CCN. Equation (11) is valid to −700°C, the limit of calculations made. It is also valid for SW = 0.82 to 0.999.

One factor not considered in this parameterization is that only the smaller nuclei for cloud condensation achieve their equilibrium radii as relative humidity approaches 100% (e.g., Mordy 1959). It is clear upon considering typical cirrus cloud vertical velocities that nonequilibrium considerations are important for soluble particles with mass larger than about 10^{-13} g. Ignoring this effect in the parameterization may lead to some overestimate of nucleation rates. We hope to include nonequilibrium effects in future treatments based on empirically relating haze particle growth in an explicit cloud model to updraft velocity and solute diameter D_s.

The results given by (11) are in a form that may be integrated over a generalized CCN size distribution. The exponential form of the gamma distribution (Marshall–Palmer) was used to represent dry CCN in this paper. Geometric mean diameter was selected to crudely approximate a background dry CCN particle size distribution in the upper troposphere based on past measurements of CCN supersaturation spectra. This distribution is shown in Fig. 3. The distribution given by Heymsfield and Sabin (1989) is shown for comparison. The third distribution shown in Fig. 3 is discussed later. In all distributions, we have assumed a largest mass category of 10^{-12} g, which equates to a maximum particle diameter D_{max} of 1.02 μm. For an assumed exponential CCN distribution, the total

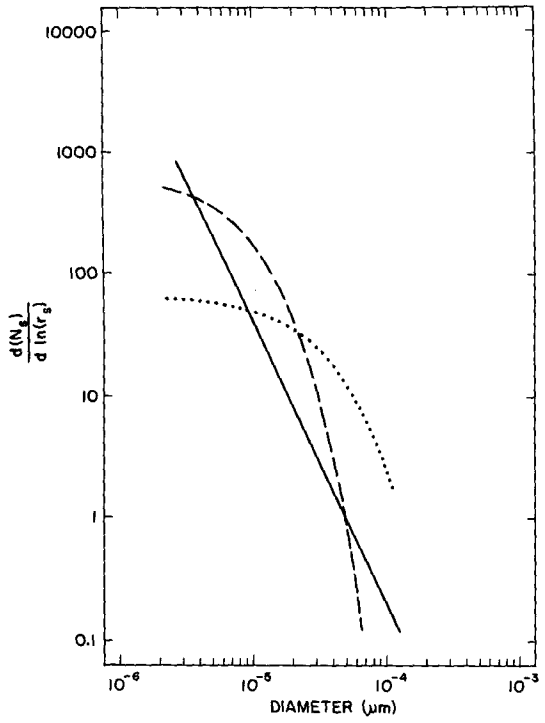

FIG. 3. Soluble particle size spectra assumed to represent natural cirrus cloud background (dashed), and a volcanically perturbed condition (dotted) for this study. The solid line represents the dry particle sizes inferred from the CCN spectra used by Heymsfield and Sabin (1989).

number concentration of haze particles freezing N_f in time step Δt may be written as

$$N_f = N_{\Delta t} \int_0^{y_{\max}} \exp(-y)\left\{1 - \exp\left[-y^b\left(\frac{D_n}{D_m}\right)^b\right]\right\} dy, \tag{12}$$

where

$$y = D/D_n.$$

In this equation, D_n is the scaling diameter, equal to 7.5×10^{-6} cm here, and D_m is defined such that $a = D_m^{(-b)}$; N_t is the total CCN concentration taken here to be the same as the concentration parameter of the CCN spectrum (200 cm^{-3}). Although an analytical solution is probably possible, we chose to numerically integrate (12) for the model sensitivity studies which follow. A table was thereby created to express N_f versus temperature and relative humidity for use in the mesoscale cloud model. A relationship between N_f and the ratio (D_n/D_m) also results from integration. This could readily be approximated by a combination of two polynomials with high confidence for use in the parcel model simulations. Freezing nucleation was only permitted above the deliquescence point (82% relative humidity).

3. Numerical model sensitivity studies

In order to demonstrate some implications of the homogeneous freezing nucleation parameterization and to investigate interactions with heterogeneous nucleation processes, some sensitivity simulations were performed using a detailed microphysical parcel model. We also present a 2D sensitivity simulation with a regional-scale cloud model, initialized with a horizontally homogeneous sounding.

a. Parcel model

1) DESCRIPTION

The parcel model used is a modified version of the model described by Rokicki and Young (1978), a derivative of the 2D microphysical model described in detail by Young (1974a). This model permits an analysis of the performance of the parameterization versus the more explicit calculations, and it gives insight into the competitive nature of the homogeneous and heterogeneous ice formation processes in cirrus clouds.

Key features of the parcel model in regard to this study are that particle temperatures are calculated explicitly, precipitation does not occur from the parcel, and, except for a specification of vertical motion, cloud dynamics is not considered. The model is thus most appropriate simply for studies of the initiation of ice and precipitation. The natural nucleation routines have been greatly modified for this and recent other studies, as now described.

Condensation nucleation is predicted based on specified CCN spectral concentration (C) and power (K) coefficients. In this study the same coefficients were used for droplet activation as were used to determine the dry hygroscopic particle size spectrum used for computing haze particle freezing rates. These were C = 200 cm^{-3} and K = 1.5. New droplets enter as 2.1-μm radius particles and are transferred during growth through 48 size categories up to several millimeters.

Heterogeneous ice formation follows from three schemes that quantify four ice formation mechanisms. The deposition/condensation freezing model of Meyers et al. (1992) is used to describe nucleation from the vapor state below and above water saturation. This model is based on data from continuous flow diffusion chambers relevant to both deposition nucleation and the sorption form of condensation-freezing. Ice crystal concentrations are specified as a function of the ice supersaturation. In the parcel model, new ice is formed by this mechanism only when the supersaturation exceeds the highest value from previous time steps.

A natural immersion freezing routine was not used in this study. There is reason to believe that the activity of this natural IN population is already accounted for within the Meyers et al. (1992) deposition and condensation freezing nucleation parameterization. Also, calculations of expected ice crystal concentrations nu-

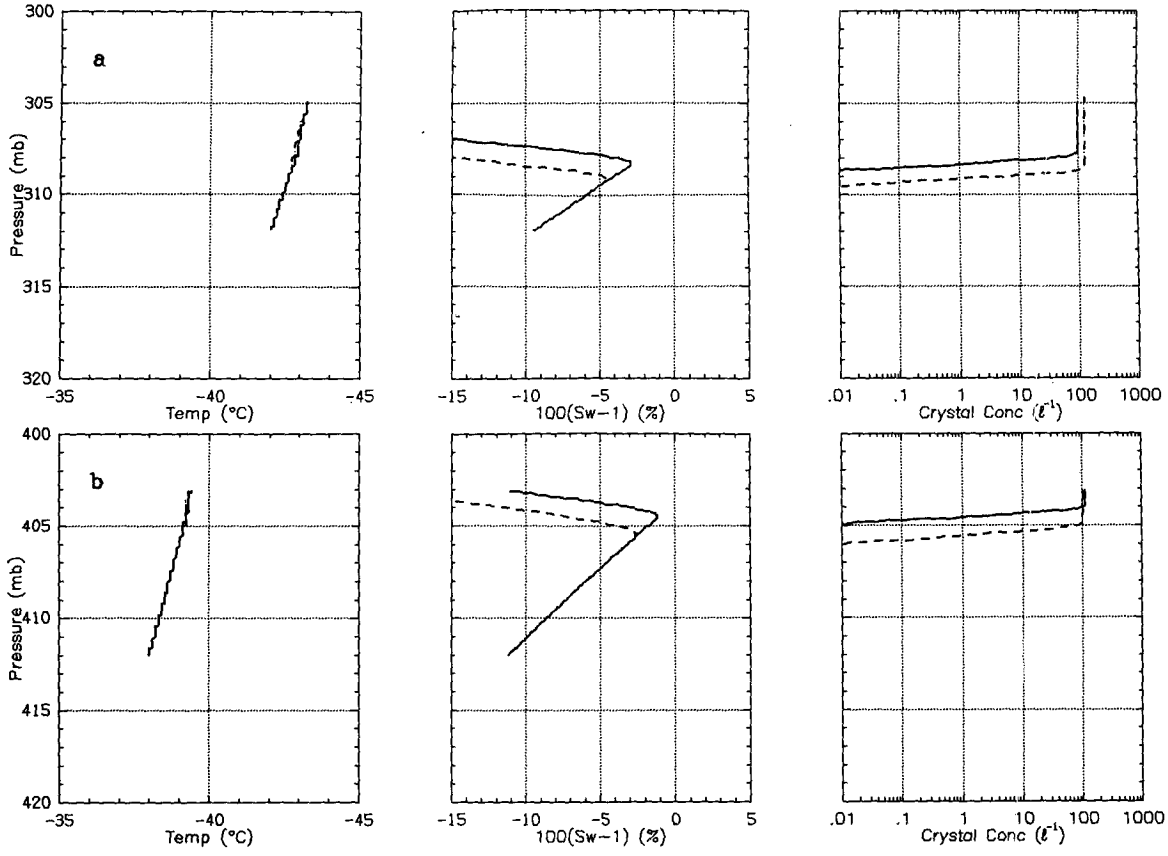

FIG. 4. Temperature, water supersaturation, and ice crystal concentration formed by homogeneous freezing as parameterized (dashed) and as calculated more explicitly (solid line) in 5 cm s^{-1} updraft simulations with the parcel model. Initial temperature is −42°C in (a) and −38°C in (b).

cleated by the heterogeneous droplet freezing mechanism for cirrus cloud conditions showed this process to be of minor importance compared to the homogeneous freezing process and other heterogeneous mechanisms. This is because the rate of the homogeneous freezing process is much faster for haze-sized drops and because cloud droplets stay very small when they are formed at cirrus temperatures.

Contact freezing nucleation activity in the parcel model is from Meyers et al. (1992), based on an accumulation of various laboratory data for natural aerosols. The fraction of the activity realized in any time step is determined by the collection rates of ice nuclei by cloud droplets due to the combined effects of Brownian collection, thermophoresis, diffusiophoresis, and aerodynamic capture. Calculations of collection rates follow the equations from Young (1974b) and a specification of the natural particle size distribution (15 bins). Freezing occurs at the droplet temperature.

Ice crystals nucleated from the vapor enter as 1.6-μm particles, while ice formed by freezing enters at the frozen droplet size. Ice crystals grow isometrically until a semiaxis of 20 μm is exceeded. Relative axial growth rates and densities for larger crystal sizes are determined by temperature and vapor density based on empirical data.

2) RESULTS

Numerous simulations were performed with the parcel model. A 1-s time step was used for all parcel model simulations reported herein. Heterogeneous ice formation mechanisms were deactivated for initial comparative simulations of explicit and parameterized results, and for demonstrating the character of predicted ice formation for a range of cirrus cloud conditions due only to the homogeneous process. Figure 4 compares the evolution of various cloud properties using the parameterization and the full equations, respectively, for a 5 cm s^{-1} updraft initiated at the CCN deliquescence point (82% relative humidity) at −42°C and 312 mb (Fig. 4a). Plotted versus pressure are temperature, water supersaturation, and ice crystal concentration. While initial ice formation occurs 0.1°C warmer in the parameterized simulation, no significant differences compared to the explicit results are noted. In particular, the maximum ice crystal concentrations

achieved in the two parcels are equivalent at near 100 L^{-1}. Simulations at a 5 cm s^{-1} ascent rate, but at an initial temperature of −38°C and a pressure of 412 mb, show similar excellent agreement between ice initiation by homogeneous freezing as parameterized and calculated more explicitly (Fig. 4b). These results also demonstrate the expected lower maximum humidity achieved as temperature decreases. Excellent agreement between the two methods was obtained for both lower and higher parcel ascent rates and for different temperature regimes.

The simulation results also show that maximum ice crystal concentration by homogeneous freezing alone is most dependent on vertical velocity, and is relatively independent of temperature. Figure 5 summarizes the maximum ice crystal concentration nucleated and maximum saturation ratio achieved with respect to water as a function of five vertical velocities in a series of simulations assuming only homogeneous freezing nucleation as an ice initiation process. Symbols denote initial simulation temperatures of −38° (□), −42° (×), and −46°C (●). The lines in Fig. 5 simply connect constant updraft simulations and are not meant to be exact fits. The nature and magnitude of these results agree with those of previous studies [for example, Sassen and Dodd (1989) and Heymsfield and Sabin (1989)].

One final simulation including only the homogeneous freezing process is shown in Fig. 6 to demonstrate a situation that manifests itself in wave clouds and some deep cyclonic cloud systems. This is the production of supercooled water at temperatures at which the water will freeze homogeneously. A 3 m s^{-1} ascent simulation was initiated at −34°C. Ice forms as cloud forms at −35°C and increases in concentration as the cloud cools further. Cloud completely glaciates at just below −37°C. Concentrations of ice particles formed reaches approximately 70 cm^{-3} and the average particle diameter never exceeds 20 μm during the simulation time.

Ice crystals present and continuously nucleated heterogeneously at cirrus cloud levels could have a profound effect on the importance of homogeneous freezing nucleation. This has been addressed in a cursory manner by both Heymsfield and Sabin (1989) and Sassen and Dodd (1989). The most important natural process of concern is the deposition nucleation process, due to the large potential response to high ice supersaturations present at cold temperatures. If heterogeneous deposition IN are present at cirrus altitudes in the abundance measured in the lower troposphere and with the same dependence on humidity, then the homogeneous freezing process could be irrelevant.

One must consider, however, if it is appropriate to maintain a uniform profile of potential natural ice nuclei in the vertical for cirrus cloud simulations. To investigate scenarios of the interplay between heterogeneous and homogeneous ice formation processes, parcel model simulations were performed in which the profile of potential heterogeneous ice nuclei were presumed to be either constant or to decrease with altitude. A relative decrease is expected based on the relative decrease of total aerosol concentrations with altitude in the free troposphere and based on past studies which measured vertical IN profiles (e.g., McPartland and Super 1977). In generalizing such a result, we utilize the fact that while few studies have found a relationship between total aerosol concentration and IN concentration, some past IN observations have indicated a strong relationship between IN concentration active for one set of conditions and the large mode of the total aerosol size distribution (Georgii and Kleinjung 1967; Berezinskiy et al. 1986). The relationship is very nearly linear, and we will assume it to be so. Vertical profiles of large aerosols ($D_a > 0.6$ μm) in the troposphere are not available in abundance, but typical background measurements over continental regions (Pruppacher and Klett 1978; Hofman 1988) show a decay of large aerosols from about 10 cm^{-3} at the sur-

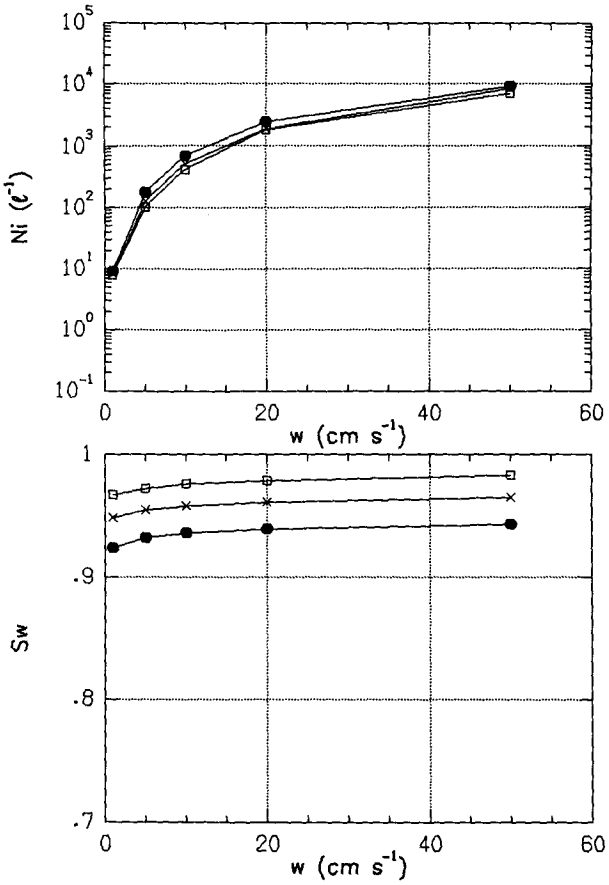

FIG. 5. Maximum ice crystal concentration nucleated and maximum saturation ratio with respect to water as a function of vertical velocity in parcel model simulations including only homogeneous freezing nucleation. Initial temperatures of −38° (open squares), −42° (crosses), and −46°C (dots) are indicated.

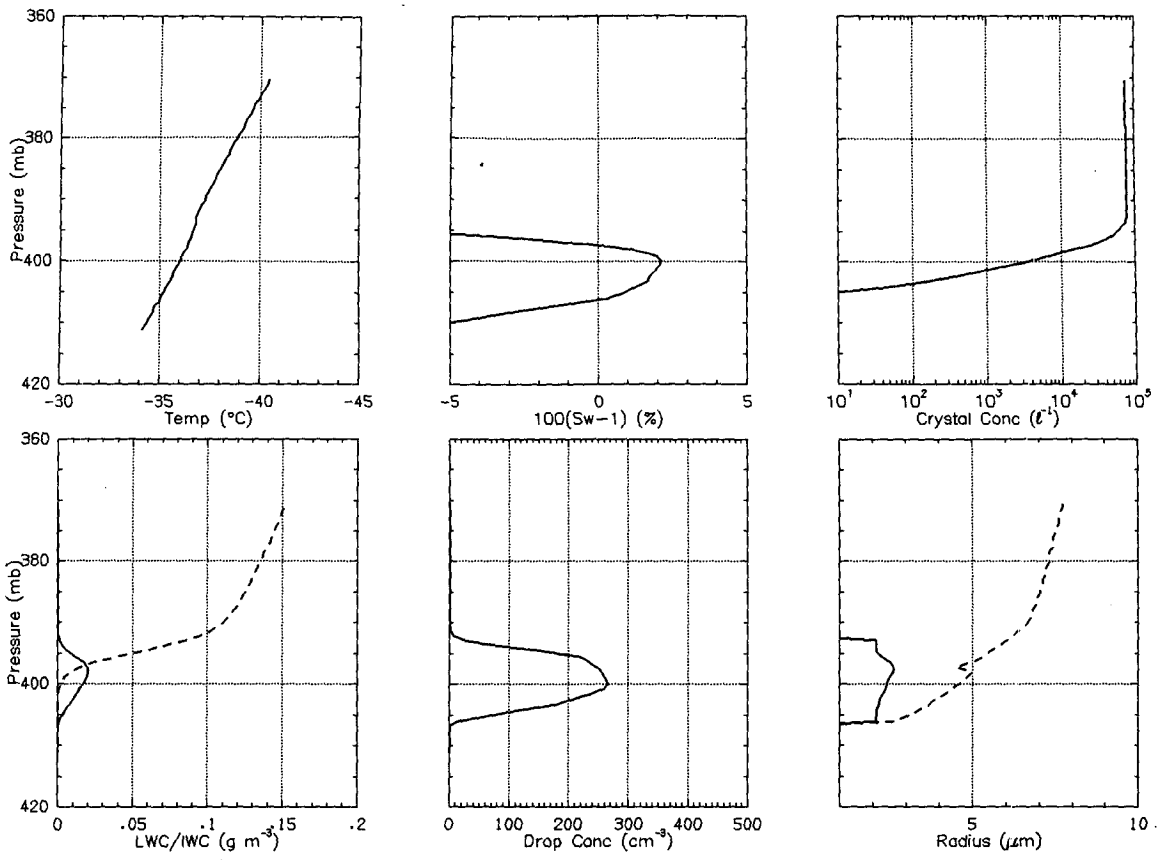

FIG. 6. Parcel model simulation of wave cloud formation (3 m s^{-1} updraft) at about −35°C, and subsequent ice formation by homogeneous freezing nucleation. Water content and particle radii are distinguished for liquid (solid line) and ice (dashed) phases.

face to <0.1 cm^{-3} at the tropopause. The decrease is nearly log linear in height, except as modified by boundary-layer mixing, inversion layers, and natural or man-made events such as volcanic eruptions and large-scale fires. Here we assume a mixed boundary layer 2-km deep with 10 cm^{-3} large aerosols and propose a decay of tenfold per 5 km in a standard atmosphere. We then relate the fraction of ice nuclei available at any height with respect to the number available at ground level to standard air density for use in modeling instances that deviate from the standard atmosphere. The polynomial expression fit to this result is given by

$$F_{IN} = -215.736 + 1.529 \times 10^{6}\rho_a - 3.455 \times 10^{9}\rho_a + 2.857 \times 10^{12}\rho_a, \quad (13)$$

where ρ_a is air density. We believe this formulation to be preferable to a simple temperature-dependent function. Figure 7 compares the concentration of ice nuclei at 95% relative humidity as a function of standard height and temperature as given by the Meyers et al. (1992) deposition/condensation freezing nuclei formula (A), and as given by the Meyers et al. formula after imposition of the height dependence inherent in (13) (B).

Some results of using the modified IN profile in conjunction with the homogeneous freezing parameterization in parcel model simulations are shown in Fig. 8. In Fig. 8a, a constant 5 cm s^{-1} ascent is initialized at −42°C, while in Fig. 8b, the same ascent is initialized at −38°C. Initial relative humidity is 82% in both cases. These results may be compared to Fig. 4, the simulations with only homogeneous ice formation parameterized. The additional plot in Fig. 8 shows average ice crystal *a*-axis and *c*-axis radii. It is seen that the activation and growth of just a few IN per liter is sufficient at −38°C to deplete the water saturation ratio and prevent the onset of ice initiation of solution droplets homogeneously. At the lower pressure and temperature, however, fewer IN are available and two distinct cloud regions result. Lower in the cloud, a few large ice crystals predominate, while higher up the homogeneous freezing process is activated. Consequently, a bimodal ice crystal spectra is formed, with a few large ice crystals and the predominance of small newly formed crystals reflected by the decrease of the average crystal semiaxes before the humidity is rapidly driven toward ice saturation.

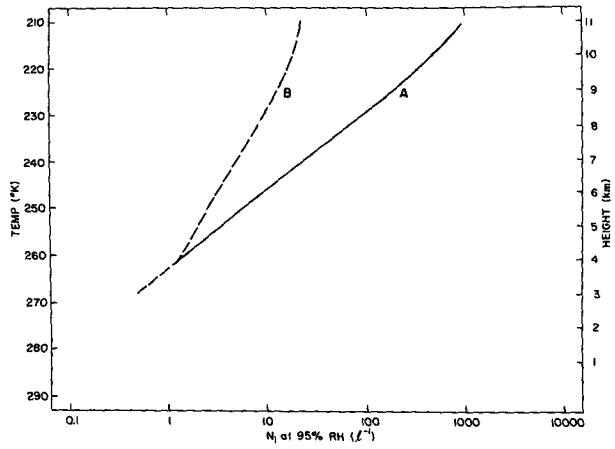

FIG. 7. Ice crystal concentration nucleated by deposition at 95% relative humidity as a function of standard temperature and height assuming no height dependence of available IN (A) and assuming that available IN decrease with height following large aerosols (B).

A number of simulations, including both homogeneous ice formation and a modified vertical profile of deposition ice nuclei, are summarized in Fig. 9. These may be directly compared to Fig. 5, the simulations using only homogeneous freezing ice formation. The addition of small numbers of heterogeneously nucleated ice crystals lowers both the maximum ice crystal concentrations and the maximum humidities achieved. These effects are particularly noted for vertical motions less than about 10 cm s^{-1}, which encompasses conditions present in many cirrus cloud systems.

It is instructive to also look at the effects of expected perturbations on background CCN and IN. One important perturbation process with regard to cirrus clouds appears to be volcanic eruptions. Sassen and Horel (1990) and Sassen (1992) have suggested that volcanic injections of aerosols into the stratosphere serve to enhance large-mode CCN aerosols in the upper troposphere by way of both long-term and short-term exchange processes. They and others (e.g., Jensen and Toon 1992) have discussed the climatic implications of volcanic CCN due to their microphysical effects on cirrus clouds. The CCN spectra given by the dotted curve in Fig. 3 are meant to emphasize the enhancement of large CCN following volcanic eruptions. The concentration of larger particles in this distribution is based loosely on observations summarized by Hofman (1988), but is quite similar to those presented by Jensen and Toon (1992). While these large particles are known predominately to be sulfuric acid, we will employ the parameterization for ammonium sulfate to crudely estimate their homogeneous freezing behavior. There may be some justification in doing so anyway because the chemical nature of these particles is likely to transform in the troposphere given the abundance of water vapor and trace gases such as ammonia. The results of simulations using the perturbed CCN spectra along with the vertically varying IN profile are summarized in Fig. 10. The implication suggested by comparing with Fig. 9 is that a large increase in the availability of large CCN in cirrus clouds does not greatly affect N_i, but permits the formation of cirrus clouds at lower humidities (about 2% lower in this case).

The conclusion obtained in the previous paragraph is much different if volcanoes, large fires, or other cataclysmic or cumulative events result in the injection of a large number of IN into the upper troposphere and lower stratosphere. While some studies of the contribution of volcanic aerosols to IN activity have given results favoring enhancement, these are not conclusive (Vali 1985). We will presume for the sake of argument that the relationship between the concentrations of large aerosols and IN concentration holds in the case of volcanic aerosols. Jensen and Toon (1992) show a size distribution of silicate-based particles that is nearly two orders of magnitude higher for large aerosols during a volcanic event than during background conditions. This suggests that a worst case scenario could be represented by the description of IN without height dependence (represented by curve A in Fig. 7). The results shown in Fig. 11 use this assumption regarding available IN along with the parameterized homogeneous freezing process as sources of ice initiation. The differences compared to other scenarios is dramatic. Maximum ice crystal concentrations are lowered and maximum humidity is lower over a wide range of typical cirrus cloud vertical motions. The homogeneous process becomes irrelevant for clouds with vertical motions less than about 30 cm s^{-1}.

Cirrus clouds are known to extend to higher altitudes and colder temperatures than we have made calculations for here. We chose not to extrapolate our results to these conditions, but there is no reason that the parameterization could not be used at colder temperatures. The essential conclusions would not change. It can be expected that with fewer heterogeneous IN available at colder temperatures assuming a vertically varying profile, ice crystal concentrations would approach the apparent limit set by the homogeneous process (Fig. 5). However, if higher numbers of deposition IN exist at colder temperatures, the saturation ratio will be driven toward the deliquescence point of pure CCN, effectively shutting down the homogeneous process. The parcel model simulations clearly indicate that heterogeneous IN potentially exert a strong microphysical influence on cirrus clouds. Lack of knowledge of background or perturbed vertical profiles of IN concentrations and their dependencies on temperature and humidity will necessarily limit our ability to model the microphysics of cirrus clouds now or for future climatic periods.

b. Mesoscale model (RAMS) sensitivity study

1) DESCRIPTION

For the 2D simulations, the Regional Atmospheric Modeling System (RAMS) was used. This model, de-

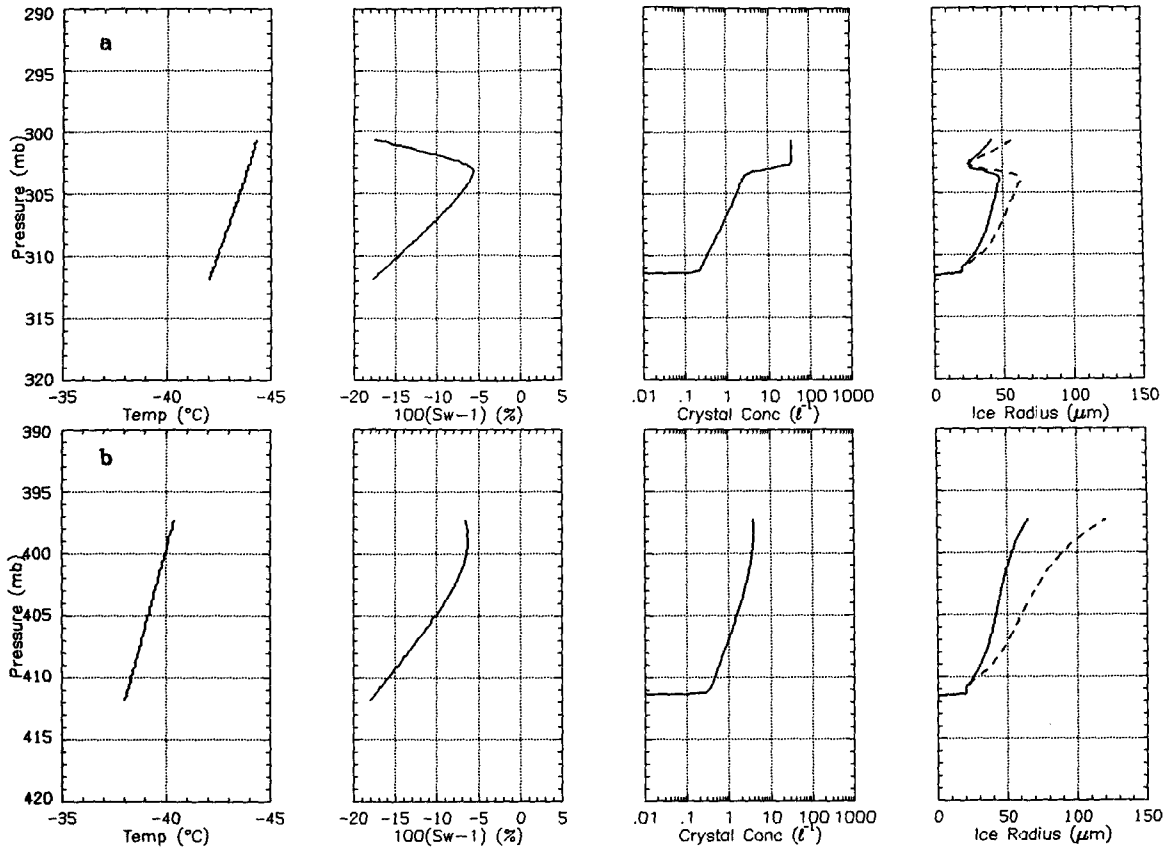

FIG. 8. Parcel model results following initialization as in Fig. 4, but permitting ice formation by homogeneous freezing and a vertically decreasing profile of heterogeneous IN. The additional panel of data includes the average ice crystal *a*-axis (solid line) and *c*-axis (dashed) radii.

scribed by Tripoli and Cotton (1982, 1989), Cram et al. (1992), Cotton et al. (1982), and Cotton et al. (1986) was developed at Colorado State University (CSU). The predicted variables include the three velocity components, the Exner function (II), the ice–liquid water potential temperature (θ_{il}) (Tripoli and Cotton 1981), pristine ice crystal concentrations, and mixing ratio of total water, rainwater, pristine ice crystals, graupel particles, and aggregates (Cotton et al. 1986). Potential temperature, temperature, cloud droplet mixing ratio, water vapor mixing ratio, and pressure are calculated diagnostically (Tripoli and Cotton 1982). A comprehensive overview of the microphysics model is given in Flatau et al. (1989). Heterogeneous ice formation occurs in the model by deposition, condensation freezing, and contact freezing nucleation as parameterized by Cotton et al. (1986) and modified by Meyers et al. (1992). The vertical profile of deposition/condensation freezing ice nuclei was modified following (13) and depicted as curve B in Fig. 7. Homogeneous freezing ice formation for cloud water was implemented following (1) and (3). Haze particle freezing follows from (12), as described in section 2b. Ice crystals are nucleated at 5 μm diameter.

A two-dimensional model domain 100 km long and 15.8 km in the vertical was used for the specific simulations presented here. The horizontal grid resolution was 1 km and the vertical grid resolution was stretched from 500 m at the surface to 50 m near 400 mb and back to 600 m above cloud level. The vertical grid increment was employed to resolve the temperature and humidity profile through the cirrus cloud layer. The model time step was 2 seconds. This is probably a realistic upper limit for the homogeneous nucleation parameterization. Since the homogeneous nucleation parameterization is a rate, there is a potential to overnucleate and deplete too much vapor with a longer time step. Therefore, a shorter time step is required.

The model was initialized with a generic sounding for a case known to produce cirrus clouds. This sounding is shown in Fig. 12. Two simulations were performed with the 2D mesoscale model: a control run that includes both heterogeneous and homogeneous nucleation and a comparison run

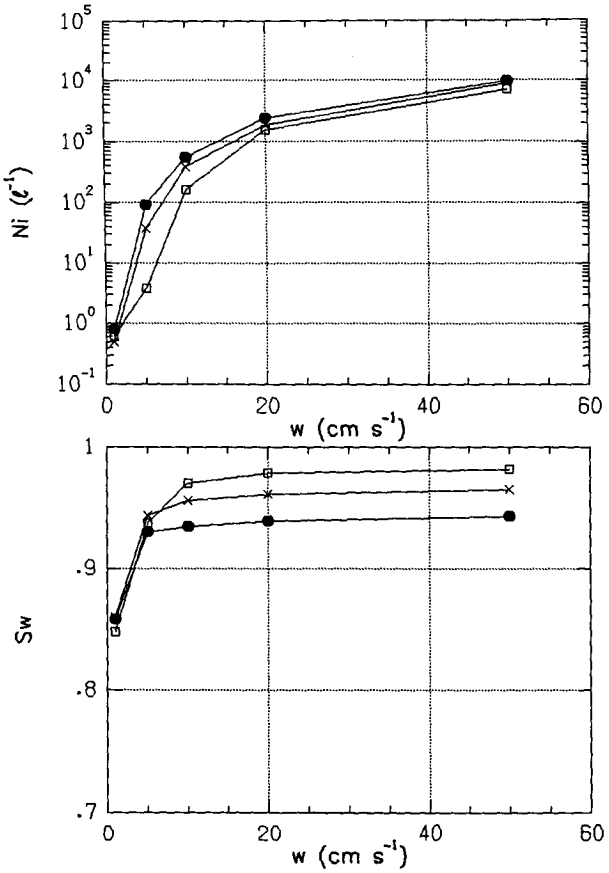

FIG. 9. As in Fig. 5 but for ice formation by homogeneous freezing and a vertically decreasing profile of heterogeneous IN.

that activates only heterogeneous nucleation processes.

2) RESULTS

Figure 13 shows time series of pristine ice crystal concentrations from the control run and the comparison run. The control run produces much higher numbers of pristine ice crystals (peak values 170 L^{-1} during the first hour) than the comparison run (less than 10 L^{-1}). Crystal concentrations greater than 1 L^{-1} extend between 7 and 9 km MSL after 15 min and between 5 and 9 km MSL by 120 min. The comparison run shows a similar initial structure after 0.25 h, but by 120 min the ice crystal cloud is essentially contained between 5 and 7 km MSL. The lowering of cloud base in both runs is due to the fallout of the pristine ice crystals. Pristine ice crystals produced by homogeneous nucleation in the control run, however, outnumber the crystals produced by heterogeneous processes in the comparison run by over an order of magnitude near the 8 km MSL level. In the control run, therefore, there is more competition for vapor at this level. With small terminal velocities due to limited growth, the residence time of these crystals is greater, explaining why the 1 L^{-1} contour extends above 8 km MSL throughout the simulation in the control run. The fewer heterogeneously produced crystals in the comparison run grow more readily and fall faster than the homogeneously produced ice crystals. The higher layer is dehumidified, effectively shutting off additional nucleation. The pristine ice mixing ratio fields from both runs (Fig. 14) shows more mass is predicted higher and colder in the cloud in the control run, with values greater than 0.1 g kg^{-1} at 8 km MSL. As in the concentration fields, the pristine mixing ratio field from the comparison run shifts to lower altitudes in time due to lower initial nucleation rates and more efficient ice crystal growth.

These results indicate that the nucleation physics used within mesoscale models could be extremely important for accurately simulating cirrus cloud structure. Both homogeneous and heterogeneous ice formation processes should be included. Future comparison with data from natural cirrus clouds may help determine the dominant process.

4. Summary and conclusions

Descriptions of heterogeneous and homogeneous ice formation processes relevant to the numerical simu-

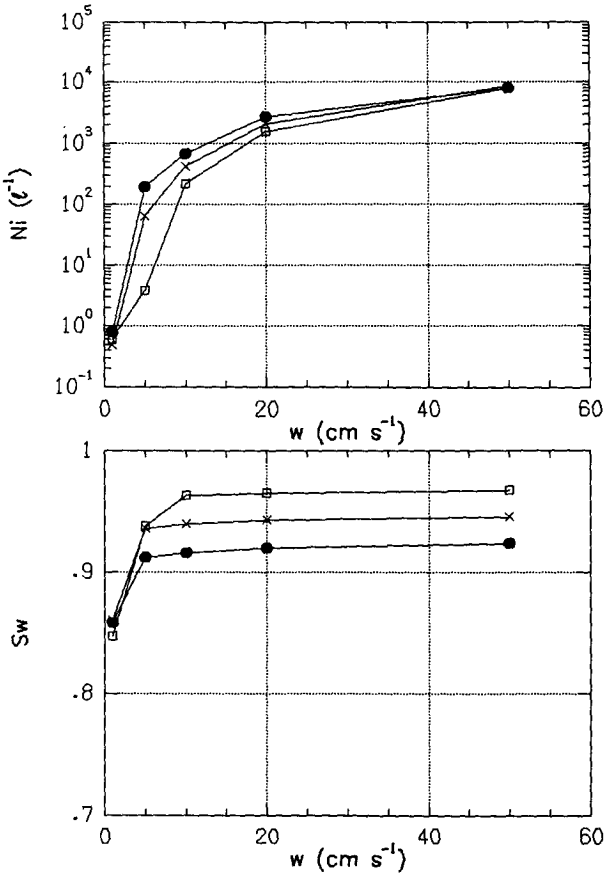

FIG. 10. As in Fig. 9 but assuming an increased population of large CCN aerosols as given by the dotted distribution in Fig. 3.

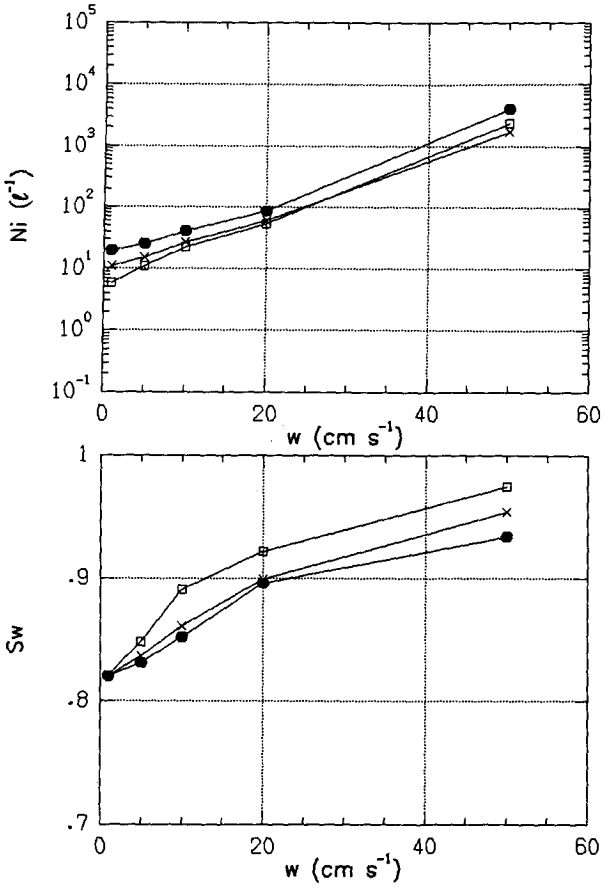

FIG. 11. As in Fig. 10 but assuming an increased population of heterogeneous IN at cirrus levels as represented by curve A in Fig. 7.

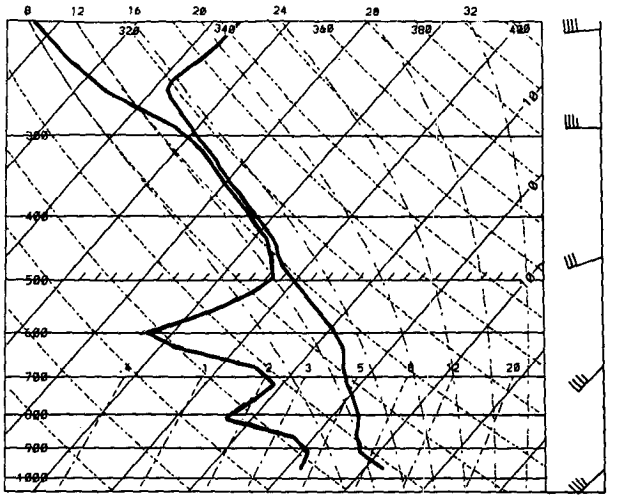

FIG. 12. Sounding used for 2D simulation.

lation of cirrus cloud microphysics have been derived for use in mesoscale cloud models. The parameterization for homogeneous freezing nucleation by haze particles includes essential dependencies on time, temperature, humidity, and CCN characteristics. The simple equations may be used with specified distributions and vertical profiles of pure CCN. Extensions of this work to include consideration of variable soluble fraction of CCN and differing CCN characteristics are straightforward. Such investigations have been made, but are not reported here because changes in these parameters do not change the conclusions regarding the interplay of homogeneous and heterogeneous ice formation processes in cirrus clouds. Parameterization of the nonequilibrium growth of larger CCN in regional-scale models is still needed.

Sensitivity experiments were performed to investigate the impact of the homogeneous freezing process on the formation and makeup of cirrus clouds. Parcel model simulations were used to demonstrate the behavior of the homogeneous freezing process. The parameterized results were in good agreement with previous studies in predicting that ice crystal concentrations nucleated below −38°C are a strong function of updraft velocity. Temperature primarily affects the maximum humidity achieved, these quantities being directly related. Very high concentrations of ice crystals are predicted to be formed in the strong vertical motions of orographic wave clouds, a point that has not

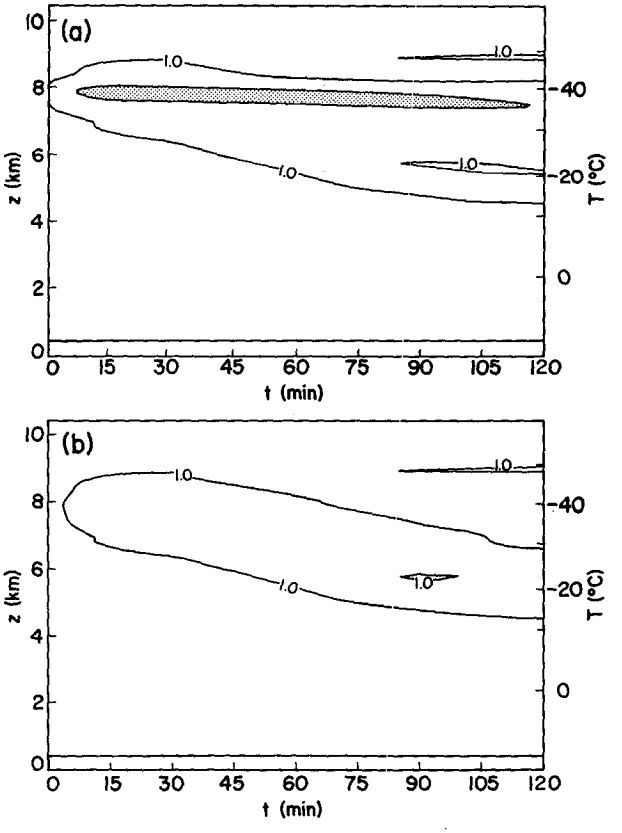

FIG. 13. A time series of pristine ice concentrations at the grid center for (a) control run and (b) the comparative run with no homogeneous nucleation processes activated. Contour interval is 1 L^{-1} with values greater than 80 L^{-1} shaded.

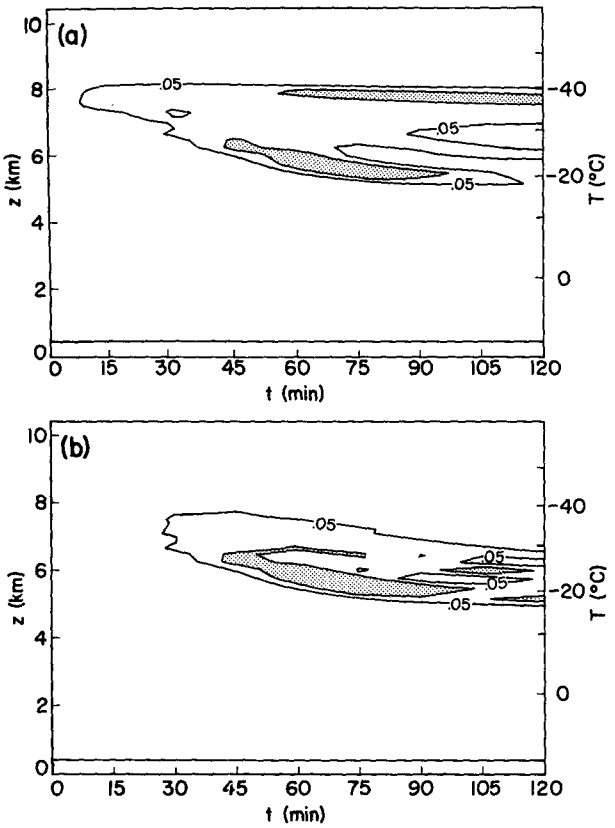

FIG. 14. Same as Fig. 13 except for pristine mixing ratio. The outer contour is 0.05 g kg^{-1}, with values greater than 0.1 g kg^{-1} shaded.

been previously emphasized. The parcel model sensitivity studies also point out the critical nature of assumptions made regarding the abundance and character of heterogeneous ice nuclei (IN) present in the upper troposphere. While the existence of supercooled water at temperatures of −30°C and colder suggests the deficiency of IN at times in the atmosphere, this cannot be taken as a general assumption. A vertical profile of IN decreasing with height was proposed as a standard background condition. Even a few background IN per liter of air were shown to greatly reduce the ice crystal concentrations and distributions, and the required humidity for cloud formation, in conditions representative of cirrus clouds.

Further sensitivity studies examined the effect of large increases of CCN and IN that can occur due to events such as volcanic eruptions. It was predicted that the introduction of additional large CCN does not affect the concentrations of ice in cirrus so much as it affects the ease with which clouds are formed. Large injections of IN typically result in clouds that form more easily and contain fewer and larger ice particles. It is clear that firm conclusions regarding the sources of ice crystals in cirrus clouds and the potential impact of nature's or of human activities on these populations must await further measurements of CCN, and particularly IN, in upper-tropospheric and lower-stratospheric regions.

A mesoscale sensitivity simulation was performed to demonstrate the implementation of parameterizations of ice formation processes in a mesoscale model and to indicate critical factors of concern for simulating microphysical and dynamic interactions in cirrus clouds. For the conditions simulated, the existence of a homogeneous freezing nucleation process led to the production of many more pristine ice crystals than in an atmosphere generally deficient in heterogeneous ice nuclei. Ice crystals produced by homogeneous ice nucleation consequently grew more slowly and had longer residence times higher in the cloud than the heterogeneously produced ice crystals. One major problem that must be faced in simulating such microphysical details in mesoscale models is the typical inadequacy of humidity profiles required for initialization. Homogeneous ice initiation is especially sensitive to small changes in the humidity profile, which is poorly represented at higher altitudes. Small vertical grid spacing may also be required to more adequately resolve humidity and ice crystal structure in cirrus cloud levels.

Acknowledgments. This research was conducted with the support of the National Science Foundation (Grants ATM8813345 and ATM-9103748), the Air Force Office of Scientific Research (Grant AFOSR-91-0269), and the Department of Defense Office of Scientific Research (Contract F49620-92-J-0331). The authors thank Dr. Piotr Flatau, Dr. Bob Walko, Dr. Johannes Verlinde, and Mr. Louis Grasso for many helpful discussions.

APPENDIX

Definition of Symbols

a_w	water activity
C	CCN supersaturation spectra concentration coefficient
D	water droplet diameter (cm)
D_a	sol droplet diameter (g)
D_s	dry solute diameter (g)
F_{hf}	fraction of CCN aerosol freezing homogeneously s^{-1}
F_{IN}	Active fraction of deposition nuclei with respect to ground-level concentrations
ΔF_{act}	activation energy for self diffusion of water (ergs)
h	Planck's constant
J_{ls}	freezing rate of solution (cm^{-3} s^{-1})
J_{ls0}	freezing rate of pure water (cm^{-3} s^{-1})
k	Boltzmann's constant
K	CCN supersaturation spectra power coefficient
L_f	latent heat of fusion (erg g^{-1})
M	molality
M_w	gram molecular weight of water
M_s	gram molecular weight of solute
m_s	mass of dry solute (g)

N_c number of monomer molecules adjacent to critical embryo
N_f total concentration (cm^{-3}) of cloud droplets freezing in Δt
N_{hf} total concentration (cm^{-3}) of haze freezing (s^{-1})
$n(D)$ droplet spectral density function
R universal gas constant per mole of dry air
S_w saturation ratio with respect to water
T_l droplet temperature (K)
T_o melting-point temperature (K)
T_{ol} average of temperatures T_o and T_l (K)
T^* effective freezing temperature (see text) (K)
ΔTm melting point (bulk freezing point) depression (K)
Δt time step (s)
V_l droplet volume (cm^3)
ν dissociation constant for solute
ϕ_s molal osmotic coefficient
ρ_l'' solution droplet density (g cm^{-3})
ρ_i average ice density between T_o, T_l (g cm^{-3})
ρ_w density of pure water (g cm^{-3})
ρ_a air density
σ_{i-w} interfacial surface tension at ice–water interface
σ_{l-a} interfacial surface tension of solution against air

REFERENCES

Berezinskiy, N. A., G. V. Stepanov, and V. G. Khorguani, 1986: Altitude variation of relative ice-forming activity of natural aerosol. *S. Meterol. Hydr.*, **12,** 86–89.

Cotton, W. R., M. A. Stephens, T. Nehrkorn, and G. J. Tripoli, 1982: The Colorado State University Three-Dimensional Cloud/Mesoscale Model-1982. Part II: An ice phase parameterization. *J. Rech. Atmos.*, **16,** 295–320.

——, G. J. Tripoli, R. M. Rauber, and E. A. Mulvihill, 1986: Numerical simulation of the effects of varying ice crystal nucleation rates and aggregation processes on orographic snowfall. *J. Climate Appl. Meteor.*, **25,** 1658–1680.

Cox, S. K., 1971: Cirrus clouds and the climate. *J. Atmos. Sci.*, **28,** 1513–1515.

Cram, J. M., R. A. Pielke, and W. R. Cotton, 1992: Numerical simulation and analysis of a prefrontal squall line. Part I: Observations and basic simulations results. *J. Atmos. Sci.*, **49,** 189–208.

DeMott, P. J., and D. C. Rogers, 1990: Freezing nucleation rates of dilute solution droplets measured between −30° and −40°C in laboratory simulations of natural clouds. *J. Atmos. Sci.*, **47,** 1056–1064.

Eadie, W. J., 1971: A molecular theory of the homogeneous nucleation of ice from supercooled water. Ph.D. dissertation, University of Chicago, Cloud Physics Lab., Tech. Note 40, 117 pp.

Flatau, P. J., G. J. Tripoli, J. Verlinde, and W. R. Cotton, 1989: The CSU–RAMS cloud microphysical module: General theory and code documentation. Atmos. Sci. Paper No. 451, Dept. of Atmos. Sci., Colorado State University, Ft. Collins, 88 pp.

Georgii, H. W., and E. Kleinjung, 1967: Relations between the chemical composition of atmospheric aerosol particles and the concentration of natural ice nuclei. *J. Rech. Atmos.*, **3,** 145–156.

Hagen, D. E., R. J. Anderson, and J. L. Kassner, Jr., 1981: Homogeneous condensation freezing measurements for small water droplets in an expansion cloud chamber. *J. Atmos. Sci.*, **38,** 1236–1243.

Heymsfield, A. J., and R. M. Sabin, 1989: Cirrus crystal nucleation by homogeneous freezing of solution droplets. *J. Atmos. Sci.*, **46,** 2252–2264.

——, and L. M. Milosevich, 1993: Homogeneous ice nucleation and supercooled liquid water in orographic wave clouds. *J. Atmos. Sci.*, **50,** 2335–2353.

Hobbs, P. V., and A. Deepak, 1981: *Clouds: Their Formation, Optical Properties, and Effects.* Academic Press, 497 pp.

Hofman, D. J., 1988: Aerosols from past and present volcanic emissions. *Aerosols and Climate,* P. V. Hobbs and M. P. McCormick, Eds., A. Deepak, 195–214.

Jensen, E. J., and O. B. Toon, 1992: The potential effects of volcanic aerosols on cirrus cloud microphysics. *Geophys. Res. Lett.*, **19,** 1759–1762.

McPartland, J., and A. B. Super, 1977: Vertical distributions of IN and CCN in Eastern Montana. *J. Wea. Mod.*, **9,** 45–50.

Meyers, M. P., P. J. DeMott, and W. R. Cotton, 1992: New primary ice nucleation parameterizations in an explicit cloud model. *J. Appl. Meteor.*, 708–721.

Mordy, W. A., 1959: Computation of the growth by condensation of a population of cloud droplets. *Tellus,* **11**(1), 16–44.

Pruppacher, H. R., and J. D. Klett, 1978: *Microphysics of Clouds and Precipitation.* D. Reidel, 714 pp.

Rasmussen, D. H., 1982: Thermodynamic and nucleation phenomena—A set of experimental observations. *J. Crystal Growth,* **56,** 56–66.

Rokicki, M. L., and K. C. Young, 1978: The initiation of precipitation in updrafts. *J. Appl. Meteor.*, **17,** 745–754.

Sassen, K., 1992: Evidence for liquid-phase cirrus cloud formation from volcanic aerosols: Climatic implications. *Science,* **257,** 516–519.

——, and G. C. Dodd, 1988: Homogeneous nucleation rate for highly supercooled cirrus cloud droplets. *J. Atmos. Sci.*, **45,** 1357–1369.

——, and ——, 1989: Haze particle nucleation simulations in cirrus clouds, and applications or numerical and lidar studies. *J. Atmos. Sci.*, **46,** 3005–3014.

——, and J. D. Horel, 1990: Polarization lidar and synoptic analyses of an unusual volcanic aerosol cloud. *J. Atmos. Sci.*, **47,** 2881–2889.

Stephens, G. L., S. Tsay, P. W. Stackhouse, Jr., and P. J. Flatau, 1990: The relevance of the microphysical and radiative properties of cirrus clouds to climate and climate feedback. *J. Atmos. Sci.*, **47,** 1742–1753.

Taborek, P., 1985: Nucleation in emulsified supercooled water. *Phys. Rev.*, **32,** 5902–5906.

Tripoli, G. J., and W. R. Cotton, 1981: The use of ice-liquid water potential temperature as a thermodynamic variable in deep atmospheric models. *Mon. Wea. Rev.*, **109,** 1094–1102.

——, and ——, 1982: The Colorado State University Three-Dimensional Cloud/Mesoscale Model—1982. Part I: General theoretical framework and sensitivity experiments. *J. Rech. Atmos.*, **16,** 186–219.

——, and ——, 1989: Numerical study of an observed orogenic mesoscale convective system. Part I. Simulated genesis and comparisons with observations. *Mon. Wea. Rev.*, **117,** 273–304.

Vali, G., 1985: Atmospheric ice nucleation—A review. *J. Rech. Atmos.*, **19,** 105–115.

Weast, R. C., Ed., 1981: *CRC Handbook of Chemistry and Physics,* 61st ed. CRC Press, 2463 pp.

Young, K. C., 1974a: A numerical simulation of wintertime orographic precipitation: Part I. Description of model microphysics and numerical techniques. *J. Atmos. Sci.*, **31,** 1735–1748.

——, 1974b: The role of contact nucleation in ice phase initiation in clouds. *J. Atmos. Sci.*, **31,** 768–776.